ELSEVIER

Journal of Nuclear Materials 248 (1997) 435–438

journal of nuclear materials

Application of synchrotron radiation to analysis of local structures in energy-related materials

Tsuneo Matsui [a,*], Tatsuya Tokunaga [a], Takanori Nagasaki [a], Yuji Arita [a], Hirotake Shigematsu [a], Taikan Harami [b], Hideo Ohno [b], Katsumi Kobayashi [c]

[a] *Department of Quantum Engineering, Graduate School of Engineering, Nagoya University, Chikusa-ku, Nagoya 464-01, Japan*
[b] *Department of Synchrotron Radiation Researches, Japan Atomic Energy Research Institute, Kamigori, Ako-gun, Hyogo 678-12, Japan*
[c] *Photon Factory, National Laboratory for High Energy Physics, Tsukuba, Ibaraki 305, Japan*

Abstract

Our recent results on the local structures around a specified atom in several kinds of energy-related materials, i.e., Mg doped UO_2 as a new type of nuclear fuel, $(La_{1-x}M_x)_2Zr_2O_7$ (M = Nd or Ce) as a promising ceramic matrix for fixation of TRU elements, and $La_2(Zr_{1-x}Y_x)_2O_7$, $Ba(Ce_{1-x}Y_x)O_3$ and $Sr(Ce_{0.95}Yb_{0.05})O_3$ as a protonic conductor, determined by EXAFS using synchrotron radiation are summarized in relation to their anticipated functional properties. © 1997 Elsevier Science B.V.

1. Introduction

The chemical and physical properties of energy-related materials have been modified by doping aliovalent cations, so as to produce several kinds of defect structures. Although the defect structures have been studied by many methods, such as X-ray and/or neutron diffraction, electrical conductivity measurement, thermogravimetry, electromotive-force measurement, etc., the local structures around the dopants with emphasis on the non-stoichiometry have not been well clarified. The information on the local structures is very important for understanding and predicting the functional properties of energy-related materials.

In the present paper, our recent results on the local structures around a specified atom in several kinds of energy-related materials, i.e., Mg doped UO_2 as a new type of nuclear fuel, $(La_{1-x}M_x)_2Zr_2O_7$ (M = Nd or Ce) as a promising ceramic matrix for fixation of TRU elements, and $La_2(Zr_{1-x}Y_x)_2O_7$, $Ba(Ce_{1-x}Y_x)O_3$ and $Sr(Ce_{0.95}Yb_{0.05})O_3$ as a protonic conductor, determined by EXAFS using synchrotron radiation are summarized in relation to their anticipated functional properties.

2. Experimental

2.1. EXAFS experiment

The local structures around the specified atoms such as the bonding length (interatomic distance), the coordination number and the distribution (movement) of defects were determined from the peak position, the peak height and the peak width of the radial structural functions, respectively, obtained by a Fourier transform of the EXAFS (extended X-ray absorption fine structure) spectrum. The X-ray absorption measurement near a specified atom was made at room temperature with synchrotron radiation by use of the EXAFS facilities on the beam lines 6B, 7C and 27B of 2.5 GeV storage ring at the Photon Factory of the National Laboratory for High Energy Physics. The X-ray absorption near edge structure (XANES) of a specific atom was also measured to determine the oxidation state of a specific atom. The continuous X-ray from synchrotron radiation was monochromatized by a silicon (311) channel-cut-crystal monochromater. The intensity of the X-ray beam before and after absorption was made for 1 s for each of the 600 points from a few hundred eV before the absorption edge to about 1 keV higher in energy.

* Corresponding author. Tel.: +81-52 789 4682; fax: +81-52 789 3779; e-mail: t-matsui@mail.nucl.nagoya-u.ac.jp.

PII S0022-3115(97)00139-6

2.2. Sample preparation and characterization

The stoichiometric sample of $(U_{0.85}Mg_{0.15})O_{2.0}$ was made by homogenizing the mixture of UO_2 and MgO_2 at 1673 K for 7 d in an Ar gas flow. The hypo-stoichiometric sample of $(U_{0.85}Mg_{0.15})O_{1.9}$ was prepared by reducing the stoichiometric one at 1273 K for 2 d in a hydrogen gas flow. The powder samples of $La_2Zr_2O_7$ and $(La_{1-x}M_x)_2Zr_2O_7$ (M = Nd or Ce) were prepared by heating the pellets made of a mixture of La_2O_3, ZrO_2, Nd_2O_3, or CeO_2 powders at 1673 K for 32 h in air and then pulverizing them. The powder sample of $Ba(Ce_{1-x}Y_x)O_3$ was made from the pellet composed of relevant binary oxides by heating at 1673 K for 35 h in air. The preparation methods of $La_2(Zr_{0.90}Y_{0.10})_2O_7$ and $Sr(Ce_{0.95}Yb_{0.05})O_3$ have been given elsewhere [1,2]. X-ray diffraction analysis indicated the presence of a single phase for each sample.

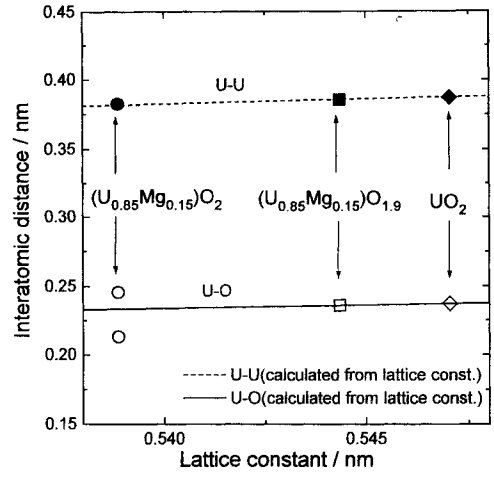

Fig. 2. Variation of the U–O and U–U interatomic distances.

3. Results and discussion

3.1. Mg doped UO_2

The local structural environment of U atoms in 15 at.% Mg doped UO_2, which is recognized as a promising nuclear fuel to control the oxygen potential in the fuel rod, was investigated in relation to the heat capacity anomaly at high temperature observed by the present authors [3]. The Fourier transformed EXAFS spectra of UO_2, $(U_{0.85}Mg_{0.15})O_{1.9}$ and $(U_{0.85}Mg_{0.15})O_{2.0}$ taken at the uranium L3 edge are shown in Fig. 1, where phase shift corrections were not made. The two main peaks attributed to the couples of U–O and U–U are seen in order of increasing distance in the Fourier spectra of UO_2 and $(U_{0.85}Mg_{0.15})O_{1.9}$, though the structure is essentially of a fluorite type. However, in the case of $(U_{0.85}Mg_{0.15})O_{2.0}$, the first peak splits into two broad peaks and the second peak is small and very broad, suggesting that there are at least two different oxygen shells around the uranium atom and the oxygen environment is not uniform. The interatomic distances obtained from the EXAFS spectra for UO_2 and Mg doped UO_2 are shown in Fig. 2 together with those calculated from the lattice constant. The coordination numbers for the nearest-neighbor oxygen shell of the uranium atom were also obtained using least-squares treatment of EXAFS spectra. In the case of UO_2, the coordination number of oxygen around uranium was calculated to be 8, but those in both $(U_{0.85}Mg_{0.15})O_{1.9}$ and $(U_{0.85}Mg_{0.15})O_{2.0}$ were larger than 8, indicating that the oxygen atoms are more favorable around the uranium atom than the magnesium atom. It is, therefore, concluded that the oxygen Frenkel defects are easily formed with increasing temperature such as to make the distributions of oxygen defects around uranium and magnesium atoms uniform (disordered), resulting in the heat capacity anomaly, consisting to the lower onset temperature (T_c) of heat capacity anomaly and the smaller enthalpy of formation of the oxygen Frenkel defects for $(U_{0.85}Mg_{0.15})O_{2.0}$ (T_c = 800 K) compared to $(U_{0.85}Mg_{0.15})O_{1.9}$ (T_c = 1150 K) determined by heat capacity measurements [3].

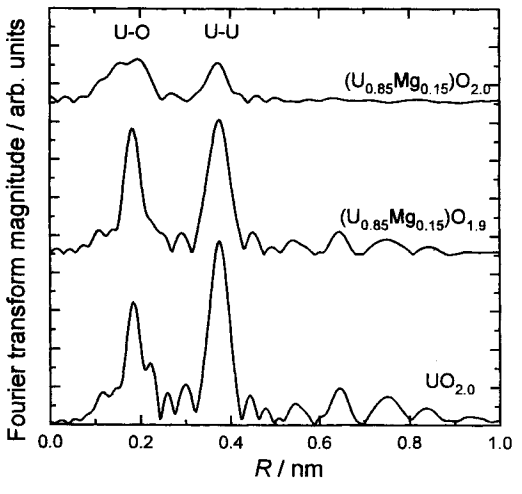

Fig. 1. Radial structural functions of the EXAFS experimental data for UO_2, $(U_{0.85}Mg_{0.15})O_{1.9}$ and $(U_{0.85}Mg_{0.15})O_{2.0}$.

3.2. $(La_{1-x}M_x)_2Zr_2O_7$ (M = Nd, Ce) and $La_2(Zr_{1-x}Y_x)_2O_7$

The pyrochlore structure containing Zr as a main constituent element with an ideal composition $M_2Zr_2O_7$ (M = tri- and/or tetravalent cations) is considered to be a candidate host matrix for fixation of high-level nuclear waste, especially lanthanides and actinide elements. The Zr–O and Zr–M (M = Zr, La and Nd or Ce) interatomic

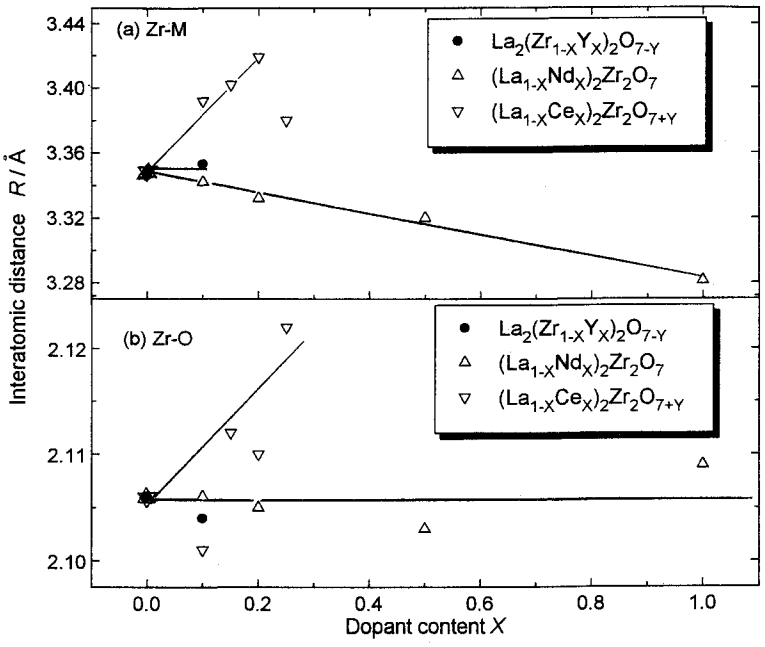

Fig. 3. The Zr–O and Zr–M interatomic distances as a function of dopant content in $La_2(Zr_{1-x}Y_x)_2O_7$, $(La_{1-x}Nd_x)_2Zr_2O_7$ and $(La_{1-x}Ce_x)_2Zr_2O_7$.

distances in $(La_{1-x}M_x)_2Zr_2O_7$ (M = Nd, Ce) obtained in this study are shown in Fig. 3 as a function of dopant content. The Zr–O interatomic distance of the Nd-doped sample is seen to be almost constant, reflecting the equal trivalent state of Nd to La. On the other hand, the Zr–O distance of the Ce-doped sample increases with increasing Ce content. The oxygen coordination number around Zr in $(La_{1-x}M_x)_2Zr_2O_7$ was also determined to increase with increasing Ce content, suggesting the introduction of interstitial oxygens located adjacent to Zr^{4+} by the addition of Ce^{4+} instead of La^{3+} from the electroneutrality condition. The predominant presence of Ce as the tetravalent state was supported from the shape of XANES at the Ce L3 edge in this study. The Zr–metal interatomic distances obtained from the second peak in the radial structural function are also shown in Fig. 3. The Zr–M interatomic distance for the Nd-doped sample decreases with increasing Nd content, but that for the Ce-doped sample increases with Ce content, also reflecting the introduction of interstitial oxygens around Zr by the addition of Ce. The A–O interatomic distances for two kinds of oxygens (8b and 48f oxygens) around the A-site (La and M site), in the pyrochlore structure calculated from the lattice constant are shown in Fig. 4. The decrease of (La, Nd or Ce)–O interatomic distances seen in this figure, suggesting the increase of the attraction (bonding strength) between cation–oxygen, is in good accordance with the experimental result of the decrease in the leaching rates of La, Nd and Ce in $(La_{1-x}M_x)_2Zr_2O_7$ in an acid solution with increasing dopant content reported by Hayakawa and Kamizono [4].

The Zr–O and Zr–(Zr, Y) interatomic distances in $La_2(Zr_{1-x}Y_x)_2O_7$, that has recently been reported as a protonic conductor [2], were also determined in this study and are also shown in Fig. 3. In the figure, both the Zr–O and Zr–(Zr, Y) distances are seen to be nearly constant. In the present EXAFS experiment, the change in La–O distance with dopant content was found to be small, and the information on the local structure around Y could not be clearly determined due to the poor absorption spectrum

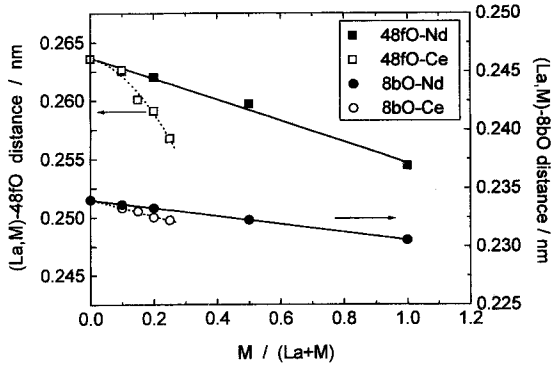

Fig. 4. The (La, M)–O interatomic distances calculated from lattice constants of $(La_{1-x}Nd_x)_2Zr_2O_7$ and $(La_{1-x}Ce_x)_2Zr_2O_7$.

near the Y–K edge. It is, therefore, thought that in the case of $La_2(Zr_{0.9}Y_{0.1})_2O_7$, oxygen vacancies introduced by the addition of trivalent Y are located adjacent to the trivalent Y with a larger ionic radius. Such location of oxygen vacancies is generally expected considering the interaction between substitutionally doped cations with a lower valence and oxygen vacancies based on the size- and electronic-effects. It is, however, noted and interesting that this location is different from that in Y-stabilized ZrO_2 with a similar structure determined by EXAFS [5], where oxygen vacancies are preferentially located adjacent to the smaller tetravalent Zr, reducing the strain between Zr and oxygens.

3.3. $Sr(Ce_{1-x}Yb_x)O_3$ and $Ba(Ce_{1-x})O_3$

The local structures of $Sr(Ce_{1-x}Yb_x)O_3$ and $Ba(Ce_{1-x}Y_x)O_3$, which are the protonic conductors [1], were also determined by EXAFS analysis. By doping Yb into $SrCeO_3$, both the Sr–O and Ce–O interatomic distances were obtained to be nearly constant. Considering the present EXAFS result and the similar ionic radius of Ce to that of Yb, oxygen vacancies introduced by doping Yb are thought to distribute uniformly around the Ce and Yb atoms, differently from the preferential location of oxygen vacancies adjacent to the Yb dopant in $Sr(Zr_{1-x}Yb_x)O_3$ [6], supporting the higher ionic conductivity of $Sr(Ce_{1-x}Yb_x)O_3$ over $Sr(Zr_{1-x}Yb_x)O_3$. The Y–O and Ba–O interatomic distances in $Ba(Ce_{1-x}Y_x)O_3$ were determined in this study as a function of Y content. Although the variations of both distances with dopant content were very small, both the minimum Ba–O distance and the maximum Y–O distance were seen at about 10% Y dopant content, where the maximum protonic conductivity has been reported [1], suggesting the largest mobility of oxygen vacancies uniformly distributed around both Ce and Y at about 10% Y content.

4. Conclusions

The conclusions obtained in this EXAFS study are summarized as follows.

(1) In Mg-doped UO_2, the oxygen environment around U atoms, i.e., U–O interatomic distance and oxygen coordination number, were not uniform and different from that around Mg atoms. This non-uniform oxygen environment is thought to be related to the easy formation of Frenkel defects of oxygen and thus to the lower onset temperature of the heat capacity anomaly of doped UO_2 over undoped UO_2.

(2) The (La, Nd or Ce)–O interatomic distances were seen to decrease with increasing dopant (M) content in $(La, M)_2Zr_2O_7$ (M = Nd, Ce), suggesting the increase of the attraction (bonding strength) between cation–oxygen. This change in the interatomic distance was in good accordance with the experimental result of the decrease in the leaching rates of La, Nd and Ce in acid solution as previously reported.

(3) Oxygen vacancies in $La_2(Zr_{0.9}Y_{0.1})_2O_7$ introduced by the addition of Y were determined to be located adjacent to the trivalent Y with large ionic radius, whose location is different from that in Y-stabilized ZrO_2 with a similar crystal structure.

(4) Oxygen vacancies introduced by Yb-doping to Sr(Ce, Yb)O_3 were seen to distribute uniformly around Ce and Yb, differently from the preferential location of oxygen vacancies adjacent to Yb in Sr(Zr, Yb)O_3, supporting the higher ionic conductivity of Sr(Ce, Yb)O_3 over Sr(Zr,Yb)O_3.

(5) The presence of the minimum Ba–O distance and maximum Y–O distance observed at about 10% Y dopant content was thought to be related to the maximum protonic conductivity.

Acknowledgements

The authors wish to express their gratitude to Professor H. Iwahara of Nagoya University for providing the pellets of $Sr(Ce_{0.95}Yb_{0.05})O_3$ and $La_2(Zr_{0.90}Y_{0.10})_2O_7$ used in this study. This work has been performed under the approval of the Photon Factory Program Advisory Committee (Proposal Nos. 95G038 and 95G233) and the program of JAERI-University Research Cooperation. This work was also supported by two Grant-in-Aids for Scientific Research 08458122 and Priority Areas, 'Dynamics of Fast Ions in Solid and Its Evolution for Solid State Ionics' No. 260 from the Ministry of Education, Science, Sports and Culture.

References

[1] T. Hibino, K. Mizutani, H. Iwahara, J. Electrochem. Soc. 140 (1993) 2588.
[2] M. Komori, H. Hayashi, T. Hibino, H. Iwahara, 20th Commemorative Int. Symp. on Solid State Ionics in Japan, Extended Abstracts, 17 (1994).
[3] Y. Arita, T.Matsui, Proc. 4th Asian Thermophys. Prop. Conf., 1995, p. 445.
[4] I. Hayakawa, H. Kamizono, Mater. Res. Soc. Symp. Proc. 257 (1992) 257.
[5] C.R.A. Catlow, A.V. Chadwick, G.N. Greaves, L.M. Moroney, J. Am. Ceram. Soc. 69 (1986) 272.
[6] T. Ousaka, Y. Kotou, H. Iwahara, 21st Annual Meeting on Solid State Ionics, 2A (12) (1995) p. 99.